

Resonance-Enhanced Intraligand and Metal–Metal Raman Modes in Weakly Metal–Metal-Interacting Platinum(II) Complexes and Long-Range Relationship between Metal–Metal Separations and Force Constants

P. D. Harvey,* K. D. Truong, K. T. Aye, M. Drouin,¹ and A. D. Bandrauk

Département de chimie, Université de Sherbrooke, Sherbrooke, Québec J1K 2R1, Canada

Received August 26, 1993[®]

The vibrational spectra (including resonance Raman) particularly in the low-wavenumber region (2–500 cm⁻¹) were investigated in the solid state at 295 K for six compounds forming either linear chains or binuclear Pt species (with or without peak Pt...Pt interactions). The $\nu(\text{Pt}_2)$ modes have been localized in the 5–55-cm⁻¹ range. For the chain compounds the data are as follows: $[\text{Pt}(\text{bpy})_2](\text{NO}_3)_2 \cdot 3\text{H}_2\text{O}$, no $\nu(\text{Pt}_2)$; $[\text{Pt}(\text{bpy})_2](\text{Pt}(\text{CN})_4)$, $\nu(\text{Pt}_2) = 54 \text{ cm}^{-1}$? (from IR); $[\text{Pt}(\text{NH}_3)_4](\text{PtCl}_4)$, $\nu(\text{Pt}_2) = 50 \text{ cm}^{-1}$; $\text{PtCl}_3(\text{DMSO})$, $\nu(\text{Pt}_2) = 5 \text{ cm}^{-1}$. For the binuclear compounds the data are as follows: $[(\text{Bu}-t\text{-NC})_2\text{ClPt}(\mu\text{-CN})\text{Pt}(\text{CN}-t\text{-Bu})\text{Cl}_2][\text{cis-Pt}(\text{CN}-t\text{-Bu})_2\text{Cl}_2]$, $\nu(\text{Pt}_2) = 38 \text{ cm}^{-1}$; $[(\text{CH}_3)\text{ClPt}(\mu\text{-Cl})(\mu\text{-Cl})(\mu\text{-Ph}_2\text{PPy})\text{Pt}(\text{CH}_3)(\text{DMSO})] \cdot \text{DMSO}$, $\nu(\text{Pt}_2) = 43 \text{ cm}^{-1}$. Using these data and 12 other literature data of compounds for which both $\nu(\text{Pt}_2)$ and $r(\text{Pt}_2)$ are known, a reparametrized Herschbach–Laurie relationship was designed ($r(\text{Pt}_2) = -0.223 \ln F(\text{Pt}_2) + 2.86$, where $F(\text{Pt}_2)$ is the force constant in $\text{mdyn } \text{Å}^{-1}$; $\sigma = 0.98$ for 16 data points). The Pt_2 data are compared with those known for the Ag_2 , Pd_2 , Rh_2 , and Au_2 systems.

Introduction

The photochemical properties of transition metal–polypyridine complexes have been a subject of intensive research in the last several years, due to their possible use in the conversion and storage of solar energy.^{2–4} Because of the metal–metal interactions in these complexes, cooperative phenomena such as high-temperature superconductivity and semiconductivity have long been predicted.^{5,6} The largest emphasis on 1-D inorganic conductors has been on the Pt compounds. As a result of the crystal structure analysis, trends of the Pt oxidation state vs Pt–Pt bond distance and conductivity have been noted.⁷ Interestingly, the sum of the r_{vdw} values is commonly accepted as being the criterion for the presence of metal–metal interactions, but an increasing amount of data in the literature tends to prove the reverse as in the case of van der Waals molecules.⁸ For the Pt element, there have been some examples for which observable Pt...Pt interactions have been noticed for quite some time despite the long $r(\text{Pt} \cdots \text{Pt})$ values. These series include complexes such as the planar D_{2h} $\text{Pt}_2\text{X}_6^{2-}$ compounds ($r(\text{Pt} \cdots \text{Pt}) = 3.418(1) \text{ Å}$, $\text{X} = \text{Cl}$;⁹ $r(\text{Pt} \cdots \text{Pt}) = 3.55(1) \text{ Å}$, $\text{X} = \text{Br}$ ¹⁰) and the linear-chain materials¹¹ (such as in the $[\text{Pt}(\text{CN})_4]^{2-}$ salts ($3.4 \leq r(\text{Pt} \cdots \text{Pt}) \leq$

3.7 Å^{12}), and $\text{cis-}[\text{Pt}(\text{en})\text{X}_2]$ complexes ($r(\text{Pt} \cdots \text{Pt}) = 3.38(3) \text{ Å}$, $\text{X} = \text{Cl}$;¹³ $r(\text{Pt} \cdots \text{Pt}) = 3.50 \text{ Å}$, $\text{X} = \text{Br}$ ¹⁴). The very few reported vibrational studies on these systems have been unable to locate the Raman-active low-frequency $\nu(\text{Pt} \cdots \text{Pt})$ modes.^{15–19} Bearing in mind that the Pt...Pt separations are close to the sum of the $r_{\text{vdw}}(\text{Pt})$ values (3.40–3.60 Å),²⁰ one should expect that the $\nu(\text{Pt} \cdots \text{Pt})$ would appear in the lattice region (20–70 cm⁻¹). Recently, Miskowski *et al.* expanded this family to the luminescent platinum(II) α -diimine complexes,²¹ which crystallize in a columnar fashion ($3.0 < r(\text{Pt} \cdots \text{Pt}) < 3.5 \text{ Å}$), and to binuclear platinum–terpyridine complexes, where the Pt...Pt distances vary from 2.998(2) to 3.342(3) Å.²² It has been demonstrated that the lowest energy excited state is MLCT-type and depends upon the metal–metal distances.²² The latter is assigned to a $d\sigma^*(\text{Pt}_2) \rightarrow \pi^*(\text{ligand})$ excited state.^{21,22}

We wish to report here the vibrational results for a series of Pt...Pt-interacting compounds, either containing the bipyridine ligand or other ligands (containing or not containing low-energy π^* orbitals). The Pt...Pt systems investigated exhibit Pt...Pt distances from 3.25 Å (Magnus' green salt) to 6.90 Å, systems where Pt...Pt interactions are either negligible or simply nonexistent.^{24,25} For the first time, evidence for weak Pt...Pt interactions for distances up to 4.22 Å will be demonstrated, and a linear

* To whom correspondence should be addressed.

[®] Abstract published in *Advance ACS Abstracts*, April 15, 1994.

- (1) Laboratoire de chimie structurale.
- (2) (a) Balzani, V.; Lenh, J. M.; Van de Loosdrecht, J.; Mecati, A.; Sabbatini, N.; Ziesse, R. *Angew. Chem., Int. Ed. Engl.* **1991**, *30*, 190. (b) Demas, J. N.; De Graff, B. A. *Anal. Chem.* **1991**, *63*, 829A. (c) Juris, A.; Balzani, V.; Barigelletti, F.; Campagna, S.; Belser, P.; Von Zelewsky, A. *Coord. Chem. Rev.* **1988**, *84*, 85. (d) *Photoinduced Electron Transfer*; Fox, M. R.; Channon, M., Eds.; Elsevier: New York, 1988; Part A.
- (3) (a) Serpone, N.; Pontenini, G.; Jamieson, M. A.; Bolletta, F.; Maestri, M. *Coord. Chem. Rev.* **1983**, *50*, 209. (b) Gafney, H. D.; Adamson, A. W. *J. Am. Chem. Soc.* **1972**, *94*, 8338. (c) Gillard, R. D. *Coord. Chem. Rev.* **1975**, *16*, 67.
- (4) Houlding, V. H.; Frank, A. J. *Inorg. Chem.* **1985**, *24*, 3664.
- (5) Interrante, L., Ed. *Extended Interactions between Metal Ions*; American Chemical Society: Washington, DC, 1974.
- (6) Keller, H. J., Ed. *Low Dimensional Cooperative Phenomena*; Plenum Press: New York, 1975.
- (7) Williams, J. M. *Inorg. Nucl. Chem. Lett.* **1976**, *12*, 651.
- (8) Huber, K. P.; Herzberg, G. *Molecular Spectra and Molecular Structure Constants of Diatomic Molecules*; Van Nostrand: New York, 1979.
- (9) Cowman, C. D.; Thibeault, J. C.; Ziolo, R. J.; Gray, H. B. *J. Am. Chem. Soc.* **1976**, *98*, 3209.
- (10) Stephenson, N. C. *Acta Crystallogr.* **1964**, *17*, 587.
- (11) Miller, J. S., Ed. *Extended Linear Chain Compounds*; Plenum: New York, 1983; Vol. 1.
- (12) (a) Krogmann, K.; Stephan, D. Z. *Anorg. Allg. Chem.* **1968**, *362*, 290. (b) Johnson, P. L.; Koch, T. R.; Williams, J. M. *Acta Crystallogr.* **1977**, *B33*, 1976. (c) Ferraro, J. R.; Basile, L. J.; Williams, J. M.; McOmber, J. I.; Shriver, D. F.; Greig, D. R. *J. Chem. Phys.* **1978**, *69*, 3871.
- (13) Martin, D. S., Jr.; Hunter, L. D.; Kroening, R.; Coley, R. F. *J. Am. Chem. Soc.* **1971**, *93*, 5433.
- (14) Kroening, R. F.; Hunter, D. L.; Rush, R. M.; Clardy, J. C.; Martin, D. S., Jr. *J. Phys. Chem.* **1973**, *77*, 3077.
- (15) Goggin, P. L. *J. Chem. Soc., Dalton Trans.* **1974**, 1483.
- (16) Hall, J. R.; Hiron, D. A. *Inorg. Chim. Acta* **1979**, *34*, L277.
- (17) Omura, Y.; Nakagawa, I.; Shimanouchi, T. *Spectrochim. Acta* **1971**, *27A*, 1153.
- (18) Berg, R. W.; Rasmussen, K. *Spectrochim. Acta* **1973**, *29A*, 37.
- (19) Nishida, Y.; Kazuka, M.; Nakamoto, K. *Inorg. Chim. Acta* **1979**, *34*, L273.
- (20) Huheey, J. E. *Inorganic Chemistry, Principles of Structure and Reactivity*, 3rd ed.; Harper & Row: Philadelphia, PA, 1983; p 259.
- (21) Miskowski, V. M.; Houlding, V. H. *Inorg. Chem.* **1991**, *30*, 4446.
- (22) Bailey, J. A.; Miskowski, V. M.; Gray, H. B. *Inorg. Chem.* **1993**, *32*, 369.
- (23) Magnus, G. *Pogg. Ann.* **1828**, *14*, 242.
- (24) Miskowski, V. M.; Houlding, V. H. *Inorg. Chem.* **1989**, *28*, 1529.
- (25) Chana, C.-W.; Che, C.-M.; Cheng, M.-C.; Wang, Y. *Inorg. Chem.* **1992**, *31*, 4874.

Table 1. List of Compounds Investigated in This Work^a

	$r(\text{Pt}\cdots\text{Pt})$	RR	R	IR	compd no.
$[\text{Pt}(\text{bpy})_2](\text{NO}_3)_2\cdot\text{H}_2\text{O}$	6.90 ^b	✓	✓	✓	1
$[\text{Pt}(\text{bpy})_2](\text{Pt}(\text{CN})_4)$	~3.3 ^c			✓	2
$[\text{Pt}(\text{NH}_3)_4](\text{PtCl}_4)$	3.25 ^d	✓	✓	✓	3
$[(t\text{-BuNC})_2\text{ClPt}(\mu\text{-CN})\text{Pt}(\text{CN-}t\text{-Bu})\text{Cl}_2]$	3.425 ^e	✓	✓		4
$[(\text{CH}_3)\text{ClPt}(\mu\text{-Cl})(\mu\text{-PPh}_2\text{Py})\text{Pt}(\text{CH}_3)(\text{DMSO})]\cdot\text{DMSO}$	3.308 ^f		✓		5
$[\text{PtCl}_3(\text{DMSO})]_n$	4.221 ^g		✓		6

^a RR = resonance Raman, R = Raman. ^b From ref 34. ^c The $r(\text{Pt}\cdots\text{Pt})$ value has been deduced from X-ray powder diffraction analysis from ref 21. ^d From ref 13. ^e This work. ^f From ref 41. ^g From ref 45.

empirical equation relating the $r(\text{Pt}\cdots\text{Pt})$ distances (2.58–4.22 Å) to the force constants, $F(\text{Pt}\cdots\text{Pt})$, will be presented.

Experimental Section

Materials. $[\text{Pt}(\text{bpy})_2](\text{NO}_3)_2\cdot\text{H}_2\text{O}$ (1), $[\text{Pt}(\text{bpy})_2](\text{Pt}(\text{CN})_4)$ (2), and $[\text{Pt}(\text{NH}_3)_4](\text{PtCl}_4)$ (3) were synthesized according to literature procedures.⁴ $[(\text{CH}_3)\text{ClPt}(\mu\text{-Cl})(\mu\text{-PPh}_2\text{Py})\text{Pt}(\text{CH}_3)(\text{DMSO})]\cdot\text{DMSO}$ (5) and $[\text{PtCl}_3(\text{DMSO})]_n$ (6) were generous gifts from Prof. F. Faraone (Università di Messina) and Prof. F. Rochon (Université du Québec à Montréal), respectively. Bipyridine was purchased from Aldrich Chemical Co. and was used as received. Table 1 lists the compounds investigated.

$[(t\text{-BuNC})_2\text{ClPt}(\mu\text{-CN})\text{Pt}(\text{CN-}t\text{-Bu})\text{Cl}_2]$ **4**. $\text{K}_2\text{-PtCl}_4$ (0.54 g, 1.3×10^{-3} mol) was dissolved in acetone (25 mL). *tert*-Butyl isocyanide (1 mL, 1.6×10^{-2} mol) was added. After 5 min of stirring at room temperature, the initial reddish brown solution turned to orange. The solution was heated at 60 °C for 30 min and then the orange solution changed to greenish yellow. The mixture was continually stirred at room temperature for another 2 h. The solution turned fluorescent yellow. The solvent was removed, and the product was precipitated from an acetone/pentane mixture. The product was isolated in 90% yield as a fluorescent yellow solid. The crystals were grown from an acetone/pentane mixture. The product has been identified by X-ray crystallography. IR (KBr): 2217 cm^{-1} (br; $\nu(\text{CN})$). ¹H-NMR ($\text{CD}_3\text{-CN}$): 1.5–1.6 ppm (complex).

Instruments. The Raman spectra were measured on two different spectrometers. In the first case, the spectra were measured at 90° scattering and with a power lower than 10 mW at the crystals (resonance Raman; compounds 1–3). The lasers used were Spectra Physics argon and krypton ion lasers; the double monochromator was a Jobin-Yvon Ramanor (HG2S(f/7.8)); the photomultiplier was a Hamamatsu R649, cooled to 20 °C, at which temperature the photon count was 5 counts/s. Raman spectra were recorded with a 3.0- cm^{-1} spectral slit width. The second instrument was a microRaman for compounds 4–6 and was an Instruments SA Raman spectrometer equipped with a U-1000 Jobin-Yvon 1.0-m double monochromator using either the 647.1-nm red line or the 514.5- or 488.0-nm line of the Spectra-Physics krypton or argon ion laser, respectively, for excitation. For infrared work, the far-infrared spectra were taken with an FTIR BOMEM Model DA 3.002; the sample was ground and compacted with a polyethylene disk; the spectra in the region 600–3700 cm^{-1} were taken with a Perkin-Elmer Model 781 spectrophotometer, and samples were examined as KBr disks. The absorption spectra were measured on a Hewlett-Packard 8452A diode array spectrophotometer.

Crystallographic Data. The data were collected on an Enraf-Nonius CAD-4 diffractometer using graphite-monochromated $\text{Mo K}\alpha$ radiation ($\lambda = 0.71073$ Å), and the ω -scan method was used. The NRCVAX²⁶ system was used for all calculations. Direct methods followed by Fourier synthesis were used to locate all non-hydrogen atoms. The Pt and Cl atoms were treated anisotropically, while the C and N atoms were treated

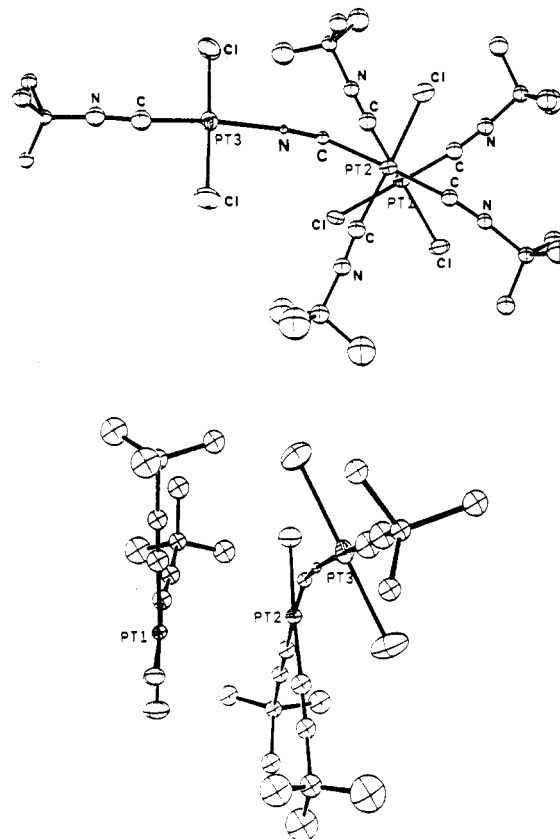


Figure 1. ORTEP^{26e} drawing for compound 4. The H atoms are omitted for clarity.

isotropically. The crystallographic data and the final coordinates and B values for non-H atoms with esd's are all presented in the supplementary material.

A yellow prismatic crystal of 4 was mounted at low temperature, and the data were collected at 190 K at a constant speed of 2.7° min^{-1} ; two standards were monitored every 30 min where no decay was noticed. Crystal data: $M = 1204.17$, orthorhombic (No. 61), $Pbca$, $a = 11.498(3)$ Å, $b = 23.289(3)$ Å, $c = 29.753(3)$ Å, $Z = 8$, $D_{\text{calc}} = 2.008$ g cm^{-3} , $\mu = 109.8$ cm^{-1} . The lattice parameters were refined from 24 reflections in the range $2^\circ \leq 2\theta \leq 45^\circ$. A total of 5143 unique reflections were measured, of which 2960 were considered to be observed with $I_{\text{net}} \geq 3.0\sigma(I_{\text{net}})$. No solvent molecule was observed in the lattice.

Results and Discussion

Structure Description. During the course of the investigations, the new compound $[(t\text{-BuNC})_2\text{ClPt}(\mu\text{-CN})\text{Pt}(\text{CN-}t\text{-Bu})\text{Cl}_2]$ (4) was prepared and characterized by X-ray crystallography, for which a brief description is now provided. 4 appears as a bright yellow and luminescent powder which crystallizes with a crystallization molecule that turned out to be a byproduct of the reaction: $\text{cis-}[\text{Pt}(\text{CN-}t\text{-Bu})_2\text{Cl}_2]$ (Figure 1). The formation of 4 involves the CN–C bond cleavage in one of the isocyanide ligands. Such a process has been reported before.²⁷ The bridging ability of a CN group is also well-known,²⁸ for which, in this case, the Pt–CN–Pt unit is not linear (the Pt–N≡C and Pt–C≡N angles are 168(3) and 173(3)°, respectively, and appear normal when compared to the data reported for $(\text{CN})_5\text{Co}(\mu\text{-CN})\text{Co}(\text{NH}_3)_5$;^{28a} the Co–N≡C and N≡C–Co angles are 159.8 and 172.4°, respectively). 4 exhibits a binuclear structure where the first Pt atom adopts the *trans*-geometry (with respect to the CN groups), while the second one exhibits the *cis*-conformation,

(26) (a) Larson, A. C. *Acta Crystallogr.* 1967, 23, 664. (b) Gabe, E. J.; LePage, Y.; Charland, J.-P.; Lee, F. L. NRCVAX: An Interactive Program System for Structure Analysis. *J. Appl. Crystallogr.* 1989, 22, 384. (c) Cromer, D. T.; Waber, J. T. In *International Tables for X-ray Crystallography*; Ibers, J. A., Hamilton, W. C., Eds.; Kynoch Press: Birmingham, England, 1974; Vol. IV, Table 2.2B, pp 99–101 (present distributor Kluwer Academic Publishers: Dordrecht, The Netherlands). (d) LePage, Y. *J. Appl. Crystallogr.* 1988, 21, 983. (e) Johnson, C. K. ORTEP: A Fortran Thermal Ellipsoid Plot Program. Technical Report 5138; Oak Ridge National Laboratory: Oak Ridge, TN, 1976.

(27) Che, C.-M.; Wong, W.-T.; Lai, T.-F.; Kwong, H.-L. *J. Chem. Soc., Chem. Commun.* 1989, 243.

(28) (a) Wang, B.-C.; Schaefer, W. P.; Marsh, R. E. *Inorg. Chem.* 1971, 10, 1492. (b) de Castello, R. A.; Mac-Loll, C. P.; Egen, N. B.; Haim, A. *Inorg. Chem.* 1969, 8, 699.

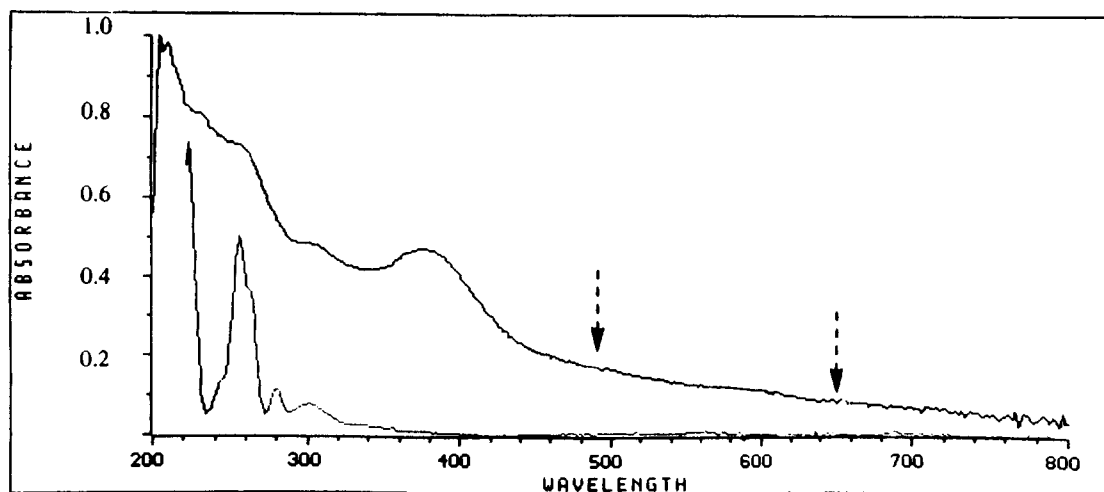


Figure 2. Comparison of the UV-visible spectra of **4** in the solid state (KBr pellet) (top) and in solution (bottom) at 298 K. Note that the baseline for the solid-state spectrum is not compensated for the diffusion of the light from the KBr pellet.

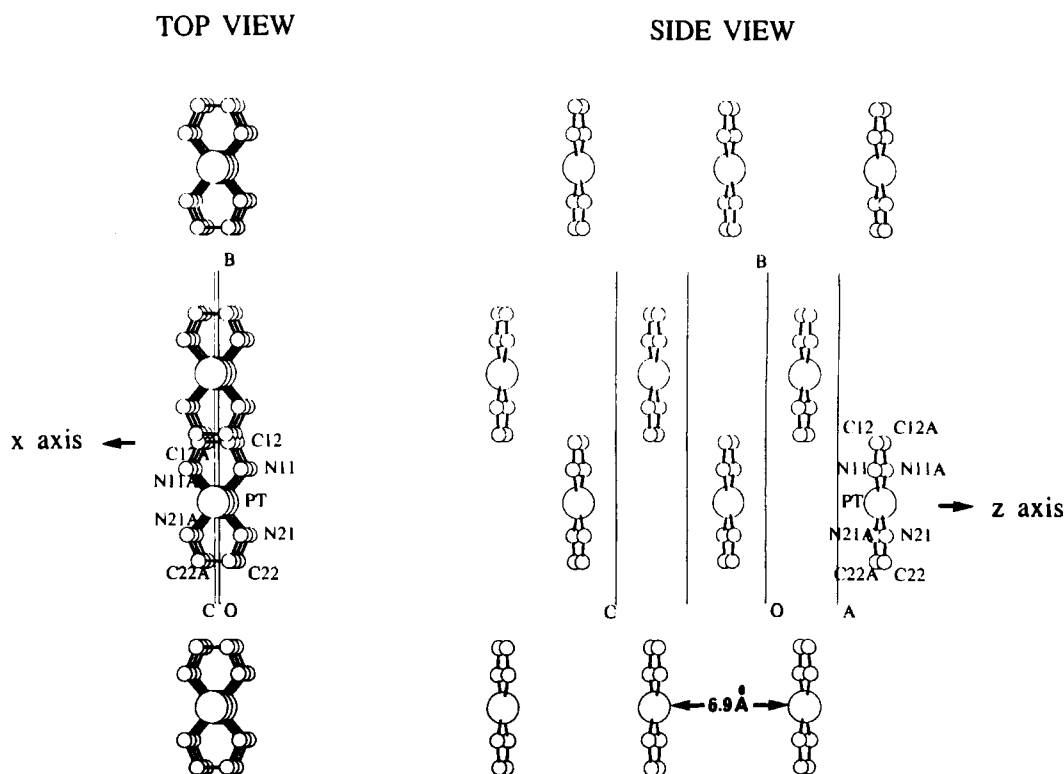


Figure 3. Views along the *a* (side view) and *c* axes (top view) for the crystal structure of **1**. The benzene groups are not completely drawn for clarity. Reprinted with permission from ref 30. Copyright 1986 American Chemical Society.

keeping two of the *t*-BuNC ligands in the axial positions of the complex (see Figure 1).

Probably due to a stacking effect, **4** is not linear, as a torsional angle (angle between the ClPtCl and ClPtCn-*t*-Bu axes) of -30.4° is observed. Of specific interest to this work, the crystallization molecule (*cis*-Pt(CN-*t*-Bu)₂Cl₂) stacks in a face-to-face fashion with the Pt atom that adopts the *cis*-geometry: $r(\text{Pt}\cdots\text{Pt}) = 3.425(3)$ Å, twist angle between the square planar moieties = 34.5° . The Pt–Cl distances for the *trans*-Pt center are 2.321(15) and 2.315(15) Å, while the $r(\text{PtCl})$ values for the *cis*-Pt species average 2.284 Å. These values appear normal. Due to the poor quality of the crystal ($R = 8.4\%$; $R_w = 10.5\%$), no other bond distance can be reported at this time (the actual data of the experiment can still be obtained from the supplementary material).

In solution, the yellow coloration vanishes completely as the UV-vis spectra exhibit bands at ~ 220 , ~ 255 , ~ 280 , and ~ 300 nm, which are associated with monomeric Pt^{II} species.²⁹ In the solid state, a broad and strong feature ranging from 360 to 400

nm ($\lambda_{\text{max}} \sim 380$ nm) is observed (Figure 2) and is indicative of Pt \cdots Pt interactions. This band is easily assigned to a $d\sigma \rightarrow p\sigma^*$ transition from the intermolecular associations of the two Pt centers (Pt1 \cdots Pt2; Figure 1). The position of this band (~ 380 nm) compares favorably to the ones reported for Pt₂(pop)₄⁴⁻ and Pt₂(pcp)₄⁴⁻ (pop = P₂O₅H₂²⁻,^{29e} $\lambda_{\text{max}} \sim 370$ nm; pcp = HO₂PCH₂PO₂H²⁻,³⁰ $\lambda_{\text{max}} \sim 382$ nm).

Vibrational Spectral Interpretation. The assignments are based upon resonance Raman enhancement effects, comparison with IR and far-IR data (notably for the $\nu(\text{Pt}_2)$ mode), comparison

- (29) (a) The three first observed bands could be assigned to $d_{z^2} \rightarrow p_z$, d_{xy} , $d_{yz} \rightarrow p_z$, and $d_{xy} \rightarrow p_z$ excitations, which are in agreement with the conventional MO scheme for square-planar d^8 complexes containing π -back-bonding ligands.^{43b-d} (b) Isci, H.; Mason, W. R. *Inorg. Chem.* **1975**, *14*, 913. (c) Isci, H.; Mason, W. R. *Inorg. Chem.* **1975**, *14*, 905. (d) Geoffroy, G. L.; Isci, H.; Litrenti, J.; Mason, W. R. *Inorg. Chem.* **1977**, *16*, 1950. (e) Isci, H.; Mason, W. R. *Inorg. Chem.* **1985**, *24*, 1761.
- (30) King, C.; Auerbach, R. A.; Fronczek, F. R.; Roundhill, D. M. *J. Am. Chem. Soc.* **1986**, *108*, 5626.

Table 2. Infrared Data (cm⁻¹) for Compounds 1, 2, and Bipyridine^a

2	1	bipyridine	assgn
54 (m)			$\nu(\text{Pt}_2)$
	64 (m)		lattice modes
80 (s)	84 (2)		+ other low
114 (s)	92 (s)		wavenumber skel
	110 (sh)		def modes
125 (s)			$\delta(\text{CPtC})$
170 (m)	160 (w)		
187 (w)	188 (w)		
210 (w)	210 (w)		
240 (w)	230 (w)		$\pi(\text{Pt-N})$
310 (w)	289 (m)		$\delta(\text{Pt-N})$
370 (w)	378 (w)		$\delta(\text{Pt-N})$
395 (s)			$\delta(\text{Pt-C}\equiv\text{N})$
430 (s)	418 (s)	400	bpy (out-of-plane ring def)
	438 (w)		
468 (m)	468 (m)		$\nu(\text{Pt-C})$
492 (m)			
658 (w)	500 (w)	617	bpy (in-plane ring def)
	655 (w)	650	
	721 (m)		ν_{NO_3}
770 (m)	775 (s)	739	CH out-of-plane
810 (w)		754	bpy bending modes
1160 (w)	1152 (w)		
	1250 (w)	1248	
1315 (w)	1320 (w)		bpy C-N str
1382 (s)			ν_{NO_3} str
1420 (w)	1428 (m)	1413	bpy ring str
1448 (m)	1450 (m)	1448	
1470 (m)	1470 (w)		ring str
1500 (m)	1500 (w)	1504	bpy C=C str
1607 (m)	1610 (s)	1554	
1645 (m)	1650 (br)	1576	bpy C=N str
	2120 (s)		$\nu(\text{C}\equiv\text{N})$
3020 (w)	3020 (w)		bpy C-H str
3040 (w)	3040 (w)	3020	
3080 (w)	3060 (w)		
3400 (br)	3460 (br)		bonded OH str

^a Key: (s) strong; (m) medium; (w) weak; (br) broad; (sh) shoulder.

with literature,³¹ and the use of empirical relationships predicting the force constant ($F(\text{M}_2)$) from $r(\text{M}_2)$, from which $\nu(\text{M}_2)$ can be extracted (for instance $\nu(\text{M}_2) = (2\pi c)^{-1}(F(\text{M}_2)/\mu)^{1/2}$).^{32,33} Compound 1 exhibits Pt...Pt separations of 6.90 Å and crystallizes in a columnar fashion (Figure 3).³⁴ The linearity of the chains is ensured from the π - π orbital overlaps of the pyridyl groups ($r(\text{C}\cdots\text{C}) = 3.45$ Å). This system is considered "monomeric" in the sense that no Pt...Pt interaction occurs. The lowest energy band has previously been assigned to arise from an intraligand (IL) (π - π^*) transition in the α -diimine complexes.²⁴ In principle, resonance Raman experiments should enhance the bipyridine ligand modes selectively; the vibrational data and spectra are given in Tables 2 and 3 and in Figures 4 and 5, respectively. No mode assignable to $\nu(\text{Pt}_2)$ could be detected in the resonance Raman experiments (Figure 5), as no particular resonance enhancement was observed, but intraligand modes were readily observed, particularly when the excitation wavelength was

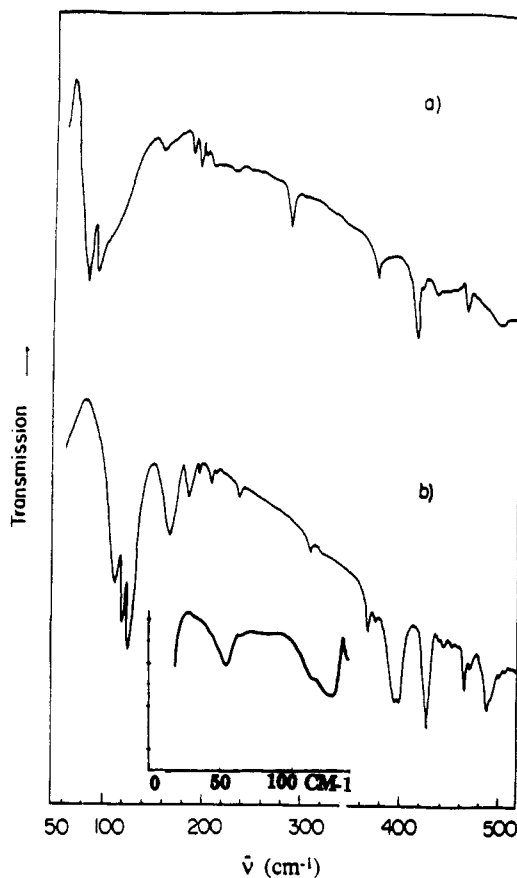


Figure 4. Comparison of the far-IR spectra for solid compounds 1 (a) and 2 (b) at 295 K. Inset: 20–140-cm⁻¹ range for 2 showing the 54-cm⁻¹ peak.

Table 3. Raman Vibrations (cm⁻¹) of Compounds 1 and 3

1	3	assgn
30		
	50	$\nu(\text{Pt-Pt})$
59		lattice modes
87	85	and other low-
96		wavenumber skel def modes
114		
	171	$\delta(\text{Pt-Cl})$
192		
255	262	$\nu(\text{Pt-N})$
	294	$\nu(\text{Pt-Cl})$
	311	$\nu(\text{Pt-Cl})$
382		bpy out-of-plane ring def
	534	$\nu(\text{Pt-N})$
656		bpy in-plane-ring def
770		
1049		
1109		$\nu_4(\text{NO}_3)$
1284		$\nu_1(\text{NO}_3)$
	1320	$\delta(\text{NH}_3)$
1324		$\nu_3(\text{NO}_3)$
1336		
1502		bpy ring str
1567		
1609		bpy C=C stretch

approaching the lowest energy band ($\lambda_{\text{max}} = 410$ nm), hence confirming the IL assignment.²⁴ The complexity of the low-wavenumber region is associated with low-wavenumber Pt(bpy) skeleton distortion and lattice modes.³¹ The far-IR region (40–200 cm⁻¹) also exhibits complex spectra for compounds 1 and 2 (Figure 4), which is not unusual for ligand-containing aromatic groups^{31b} (see also text below and refs 42 and 43).

Miskowski and Houlding²¹ have assigned the lowest energy emission transition to be $d\sigma^*(\text{Pt}_2) \rightarrow \pi^*(\alpha\text{-diimine})$ for compound 2 (and other complexes). Resonance Raman spectra in this case

(31) (a) Nakamoto, K. *Infrared and Raman Spectra of Inorganic and Coordination Compounds*, 3rd Ed.; Wiley & Sons: New York, 1986; see also references therein. (b) Turrell, G. *Infrared and Raman Spectra of Crystals*; Academic Press: New York, 1972.

(32) (a) Perrault, D.; Drouin, M.; Michel, A.; Harvey, P. D. *Inorg. Chem.* **1993**, *32*, 1901. (b) Perreault, D.; Drouin, M.; Michel, A.; Miskowski, V. M.; Schaefer, W. P.; Harvey, P. D. *Inorg. Chem.* **1992**, *31*, 695.

(33) (a) Badger, R. M. *J. Chem. Phys.* **1934**, *2*, 128; **1935**, *3*, 710. (b) Hershback, D. R.; Laurie, V. W. *J. Chem. Phys.* **1961**, *35*, 458. (c) Miskowski, V. M.; Dallinger, R. F.; Christoph, G. G.; Morris, D. E.; Spies, G. H.; Woodruff, W. H. *Inorg. Chem.* **1987**, *26*, 2127. (d) Conradson, S. D.; Sattelberger, A. P.; Woodruff, W. H. *J. Am. Chem. Soc.* **1988**, *110*, 1309. (e) Woodruff, W. H. Unpublished results.

(34) Hazell, A.; Simonsen, O.; Wernberg, O. *Acta Crystallogr.* **1986**, *C42*, 1707.

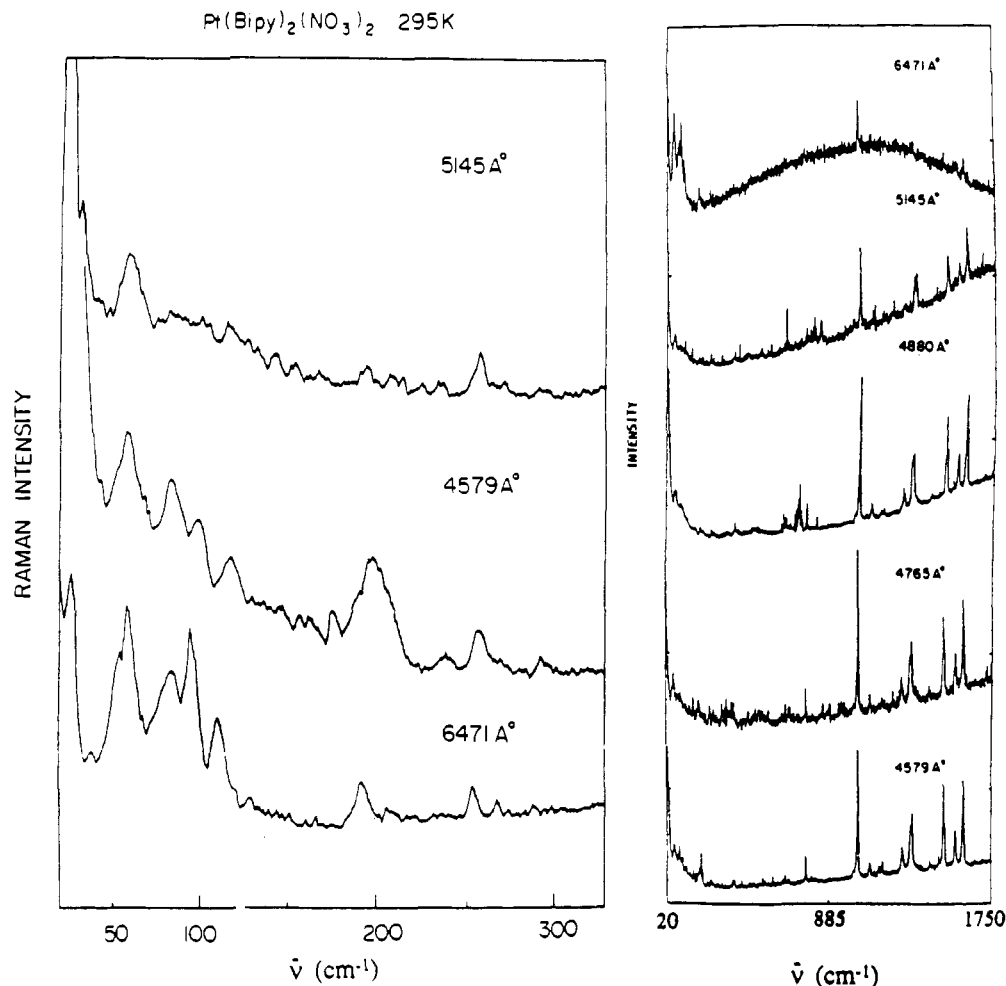


Figure 5. Resonance Raman spectra for solid compound 1, at various excitation wavelengths: 4579, 4765, 4880, 5145, 6471 Å.

should exhibit the $\nu(\text{Pt}_2)$ mode and other intraligand modes. Unfortunately, the double-salt compound 2 was too luminescent,²¹ and all attempts to obtain Raman data consistently failed. The estimated Pt...Pt separation is ~ 3.3 Å according to powder X-ray data analysis.²¹ IR data on 3 (Magnus' green salt)^{16,35} suggested that the IR-active $\nu(\text{Pt}\cdots\text{Pt})$ component (of the linear chain) should be around $80\text{--}90\text{ cm}^{-1}$. The problem with this assignment is that the IR feature at $\sim 80\text{ cm}^{-1}$ is strong and that all samples investigated in this work exhibit strong- or medium-intensity features in both the IR and Raman spectra. Furthermore, the resonance Raman spectra of $\text{Pt}_2(\text{dba})_3$ (dba = dibenzylideneacetone; $r(\text{Pt}\cdots\text{Pt}) = 3.14$ Å³⁶) conclusively placed $\nu(\text{Pt}_2)$ at 72 cm^{-1} .³⁷ At $r(\text{Pt}\cdots\text{Pt}) \sim 3.3$ Å, $\nu(\text{Pt}_2)$ should, in principle, be located at lower wavenumber ($<72\text{ cm}^{-1}$). This IR assignment for $\nu(\text{Pt}_2)$ becomes very problematic. The authors³⁵ admitted that their Raman spectra were of poor quality, where no peak was observed below 173 cm^{-1} . The Pt...Pt separation in compound 3 is similar to that in compound 2 (3.25 Å), therefore implying that $\nu(\text{Pt}_2)$ should also be similar. In this case (compound 3), the lowest energy transition is assigned to be a $d\sigma^* \rightarrow p\sigma$ transition within the Pt chain (see ref 21, page 4450). Again the $\nu(\text{Pt}_2)$ mode is also expected to be enhanced in the resonance Raman spectra. Our resonance Raman spectra for 3 show clear enhancement of the 50-cm^{-1} peak at shorter excitation wavelength (4579 Å, Figure 6). The latter is accompanied by the first harmonic at 95 cm^{-1} (coinciding with another fundamental; see spectrum at 4880 Å) and by a $\sim 145\text{-cm}^{-1}$ peak (weakly appearing in the baseline). This 50-cm^{-1} peak is therefore assigned to

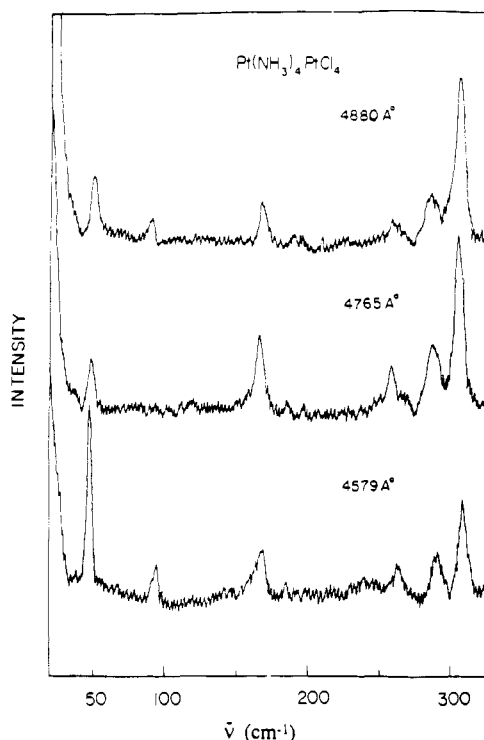


Figure 6. Resonance Raman spectra for the solid 3 (Magnus' green salt), using 4880-, 4765-, and 4579-Å laser excitation at 295 K.

(35) Adams, D. M.; Hall, J. R. *J. Chem. Soc., Dalton Trans.* **1973**, 1450.
 (36) Lewis, L. N.; Krafft, T. A.; Huffman, J. C. *Inorg. Chem.* **1992**, *31*, 3555.
 (37) Harvey, P. D.; Adar, F.; Gray, H. B. *J. Am. Chem. Soc.* **1989**, *111*, 1312.

$\nu(\text{Pt}\cdots\text{Pt})$ and compares favorably with the one for $[\text{Pt}_2(\text{en})(\text{C}_5\text{H}_4\text{NO})_2]^{4+}$ ($r(\text{Pt}_2) = 3.236$ Å,³⁸ $\nu(\text{Pt}_2) = 61\text{ cm}^{-1}$ ³⁹), also obtained

Table 4. Comparison of the Spectroscopic and Structural Properties of Weakly Interacting Heavy Diatomic Compounds (Row 5)

	$\nu(\text{M}\cdots\text{M})/\text{cm}^{-1}$	$F(\text{M}\cdots\text{M})^a/\text{mdyn}\text{Å}^{-1}$	$r(\text{M}\cdots\text{M})/\text{Å}$	$2r_{\text{vdw}}^b/\text{Å}$
3 (Magnus' green salt)	50 ^c	0.14	3.25 ^d	3.50 ± 0.10
5	43 ^c	0.11	3.308 ^e	3.50 ± 0.10
4	38 ^c	0.083	3.425 ^c	3.50 ± 0.10
Au ₂ (dmb)(CN) ₂	36 ^f	0.075	3.536 ^g	3.40
Au ₂ (tmb)Cl ₂	50 ^h	0.14	3.301 ^h	3.40
Hg ₂ (Σ _g ⁺)	18.5 ⁱ	0.020	3.63 ⁱ	3.00
Hg ₂ (Σ _u ⁺)	19.7 ⁱ	0.023	3.61 ⁱ	3.00
[Ir(μ-Pz)(COD)] ₂	58 ^j	0.19	3.216 ^k	
Ir ₂ (tmb) ₄ ²⁺	53 ^l	0.16	3.199 ^l	
Cs ₂	42.02 ^m	0.069	4.47 ^m	
HgTl	26.9 ⁿ	0.043		3.50
Xe ₂ (row 4)	22 ^m	0.019	4.36 ^m	4.40 ^o
HgXe(g)	21.18 ^p	0.021	4.05 ^p	3.70
HgCs	~30 ^m	0.042	5.09 ^m	4.15 ^q
Tl ₂ (g)	80 ^r	0.38		4.00

^a $F = \mu(2\pi\nu)^2$ for dimers. ^b Unless stated otherwise, values of van der Waals radii from: Bondi, A. *J. Chem. Phys.* **1964**, *48*, 441. Cotton, F. A.; Wilkinson, G.; Gaus, P. L. *Basic Inorganic Chemistry*, 2nd ed.; Wiley: New York, 1987; p 60. ^c This work. ^d From ref 13. ^e From ref 41. ^f From ref 32b. ^g From ref 27. ^h From ref 40. ⁱ Van Zee, R. D.; Blankespoor, S. C.; Zwier, T. S. *J. Chem. Phys.* **1988**, *88*, 4650. ^j Marshall, J. L. Ph.D. Dissertation, California Institute of Technology, 1986. ^k Coleman, A. W.; Eadie, D. T.; Stobart, S. R.; Zaworotko, M. J.; Atwood, J. L. *J. Am. Chem. Soc.* **1982**, *104*, 922. ^l Smith, D. C. Ph.D. Dissertation, California Institute of Technology, 1989. ^m Huber, K. P.; Herzberg, G. *Molecular Spectra and Molecular Structure Constants of Diatomic Molecules*; Van Nostrand: New York, 1979. ⁿ From ref 31, p 104. ^o Cook, G. A. *Argon, Helium and the Rare Gases*; Wiley: New York, 1961; Vol. I, p 13. ^p Borysow, A.; Gryark, T. *J. Phys.* **1982**, *114C*, 414. ^q This is the sum of the covalent radii (r_{cov}), since $r_{\text{vdw}}(\text{Cs})$ is unknown. Knowing that $r_{\text{cov}} < r_{\text{vdw}}$, this value is an underestimation. ^r Froben, F. W.; Schulze, W.; Kloss, U. *Chem. Phys. Lett.* **1983**, 500.

by resonance Raman spectroscopy. For the chain compound **2**, the IR-active feature located at 54 cm⁻¹ (Table 2 and Figure 4) could be associated with $\nu(\text{Pt}_2)$ on the basis of the comparison with compound **3**. Interestingly, the Au₂(tmb)Cl₂ compound (tmb) = 2,5-dimethyl-2',5'-diisocyanohexane) crystallized in a polymeric fashion with quasi-linear Au^I metals separated by 3.3063(3) Å for which $\nu(\text{Au}_2) = 50$ cm⁻¹ in the Raman spectra.⁴⁰ An IR-active feature was also reported to be at 54 cm⁻¹ for this compound (see footnote 22 in ref 40). Further to this argument, Table 6 compares the $\nu(\text{M}_2)$ and $r(\text{M}_2)$ data for the fifth-row elements with weak M₂ interactions. For data where $r(\text{M}_2) = 3.3 \pm 1$ Å, $\nu(\text{M}_2)$ is always found at values ≤ 60 cm⁻¹.

The Pt^{II}-Pt interactions at $r(\text{Pt}_2) \sim 3.3$ Å were further investigated (compound **5**; $r(\text{Pt}_2) = 3.308$ Å⁴¹). The colorless compound did not allow resonance Raman analysis, and the organometallic nature made the samples laser sensitive. The (low laser power) spectra exhibit three intense scatterings located at 43 (83%), 75 (89%), and 87 cm⁻¹ (100% relative intensity). The added complexity of this region is due to the presence of the bridging ligand PPh₂Py, which induces low-wavenumber skeleton deformation modes.^{42,43} On the basis of comparison with literature data (Table 4) and the argument stated for compounds **2** and **3**, the 43-cm⁻¹ peak is assigned to $\nu(\text{Pt}_2)$.

- (38) Hollis, L. S.; Lippard, S. J. *Inorg. Chem.* **1983**, *22*, 2600.
 (39) Stein, P.; Mahtani, H. K. In *Proceedings of the Tenth International Conference on Raman Spectroscopy*; Peticolas, W. L., Hud, B., Eds.; University Printing Department, University of Oregon: Eugene, 1986; pp 13-18.
 (40) Perreault, D.; Drouin, M.; Michel, A.; Harvey, P. D. *Inorg. Chem.* **1991**, *30*, 2.
 (41) Arena, C. G.; Bruno, G.; De Munno, G.; Rotondo, E.; Drommi, D.; Faraone, F. *Inorg. Chem.* **1993**, *32*, 1601.
 (42) (a) Raman spectra of a number of Rh₂(PPh₂Py)₂ complexes have been examined,^{42b} and invariably the lattice region is found to be complicated. Under preresonance Raman conditions, the spectra become significantly more featureless in this region. These modes are associated to lattice modes and other low-frequency skeleton torsional modes. (b) Harvey, P. D.; Shafiq, F.; Eisenberg, R. Manuscript under preparation.

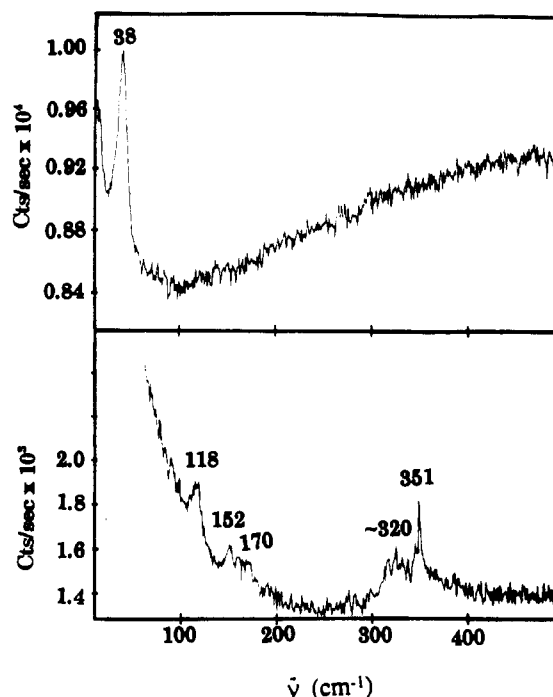


Figure 7. Top: Preresonance Raman spectrum of solid **4** at 295 K using the 4880-Å laser excitation. Experimental conditions: ~10-mW laser power at the sample, 32× microscope objective, 1 s/point, 1 point/cm⁻¹, no smoothing applied, one scan. Bottom: Raman spectrum of solid **4** using the same experimental conditions, except that the laser excitation was 6471 Å.

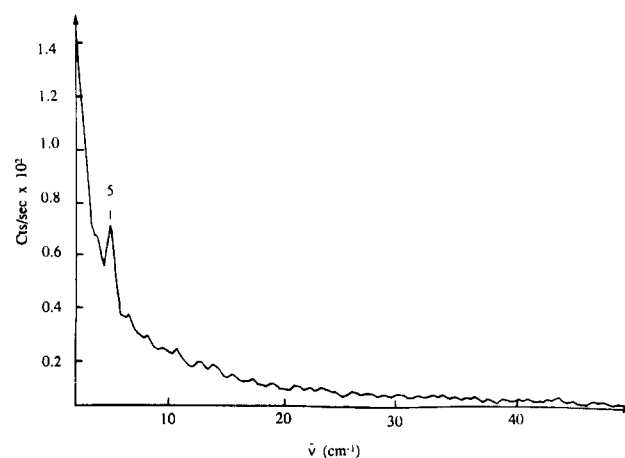


Figure 8. Solid-state Raman spectrum of compound **6** at 295 K. Experimental conditions: 514.5-Å laser excitation, 20-mW laser power at the sample, 32× microscope objective, 10 s/point, 0.5 point/cm⁻¹, no smoothing applied, one scan, slits 50 μm. The slits have to be small to allow measurements near the Rayleigh line. As a consequence, the intensity of the signal will appear small.

Preresonance Raman (4880 Å; near the $d\sigma^* \rightarrow p\sigma$ band) and (regular) Raman (6471 Å) spectra of compound **4** were obtained (Figure 7). Under preresonance conditions, an intense scattering is observed at 38 cm⁻¹ (as well as a broad luminescence) and is easily assigned to $\nu(\text{Pt}_2)$. This value compares favorably to that of Au₂(dmb)(CN)₂ ($\nu(\text{Au}_2) = 36$ cm⁻¹, $r(\text{Au}_2) = 3.536$ Å).^{27,32b} The "regular" Raman spectra exhibit weak features at 118, 152, and ~172 cm⁻¹ (deformation modes) and at ~320 and 351 cm⁻¹

- (43) (a) dppm (Ph₂PCH₂PPh₂) is an analogue of PPh₂Py. The same effect as stated in footnote 42 is observed. See for example: Alves, O. L.; Virtoso, M.-C.; Sourisseau, C. *Nouv. J. Chim.* **1983**, *7*, 231. (b) Perreault, D.; Michel, A.; Drouin, M.; Harvey, P. D. *J. Chem. Soc., Dalton Trans.* **1993**, 1365.
 (44) In the 25-500-cm⁻¹ region, the other observed Raman peaks are 105, 136, 150, 123, 216, 237, 258, 282, 289, 314, 333, 381, 444, and 463 cm⁻¹. These peaks were not interpreted due to the complexity of the molecule.

Table 5. Spectroscopic and Structural Data for Pt₂ Species

data point no.	species	$\nu(\text{Pt}\cdots\text{Pt})^a/\text{cm}^{-1}$	$F(\text{Pt}\cdots\text{Pt})^a/\text{mdyn } \text{Å}^{-1}$	$r(\text{Pt}\cdots\text{Pt})/\text{Å}$	bond order
1	6	5 (this work)	0.0027	4.221 ^a	0
2	4	38 (this work)	0.083	3.425 (this work)	0
3	5	43 (this work)	0.11	3.308 ^b	0
4	3	50 (this work)	0.14	3.25 ^c	0
5	[Pt ₂ (en) ₂ (C ₅ H ₄ NO) ₂] ₂ ⁴⁺	61 ^d	0.21	3.236 ^e	0
6	Pt ₂ (dba) ₃	72 ^f	0.30	3.14 ^g	0
7	Pt ₂ (dppm) ₃	102.5 ^k	0.60	3.025 ⁱ	0
8	Pt ₂ (pop) ₄ ⁴⁻	113 ^j	0.73	2.980 ^l	0
9	Pt ₂ (pop) ₄ ⁴⁻	118 ^k	0.80	2.925 ^l	0
10	Pt ₂ (NH ₃) ₂ (C ₅ H ₄ NO) ₂ ²⁺	139 ^m	1.11	2.898 ⁿ	0
11	Pt ₂ (pop) ₄ Cl ⁴⁻	152 ^o	(1.45) ^p	2.813 ^q	0.5
12	Pt ₂ (pop) ₄ Br ⁴⁻	120 ^o	(1.34) ^p	2.793 ^r	0.5
13	Pt ₂ (pop) ₄ (NO ₂) ₂ ⁴⁻	151 ^r	1.68 ^r	2.754 ^u	1
14	Pt ₂ (pop) ₄ Br ₂ ⁴⁻	134 ^p	1.74 ^r	2.720 ^w	1
15	Pt ₂ (pop) ₄ Cl ₂ ⁴⁻	158 ^p	1.75 ^r	2.695 ^w	1
16	Pt ₂ (dppm) ₂ Cl ₂	150 ^r	1.84 ^r	2.699 ^y	1
17	Pt ₂ (CO) ₂ Cl ₄ ²⁻	173 ^r	2.57 ^r	2.584 ^{aa}	1
	Pt ₂ (A←X), matrix 12 K	218.4 ^{bb}	2.72		?

^a From ref 45. ^b From ref 41. ^c From ref 13. ^d From ref 39. ^e Hollis, L. S.; Lippard, S. J. *Inorg. Chem.* **1983**, *22*, 2600. ^f From ref 37. ^g From ref 36. ^h Harvey, P. D.; Gray, H. B. *J. Am. Chem. Soc.* **1988**, *110*, 2145. ⁱ Manojlovic-Muir, L. J.; Muir, K. W. *J. Chem. Soc., Chem. Commun.* **1982**, 1155. Manojlovic-Muir, L.; Muir, K. W.; Grossel, M. C.; Brown, M. P.; Nelson, C. D.; Yavari, A.; Kallas, E.; Moulding, R. P.; Seddon, K. R. *J. Chem. Soc., Dalton Trans.* **1985**, 1955. ^j From ref 30. ^k Che, C.-M.; Butler, L. G.; Gray, H. B.; Crooks, R. M.; Woodruff, W. H. *J. Am. Chem. Soc.* **1983**, *105*, 5492. ^l Filomena dos Remedios Pinto, M. A.; Sadler, P. J.; Neidle, S.; Sanderson, M. R.; Kuroda, R. J. *J. Chem. Soc., Chem. Commun.* **1980**, 13. Marsh, R. E.; Herstein, F. H. *Acta Crystallogr.* **1983**, *B39*, 280. ^m Mahtani, H. K. Ph.D. Dissertation, Duquesne University, 1988; see also references therein. ⁿ Hollis, L. S.; Lippard, S. J. *J. Am. Chem. Soc.* **1981**, *103*, 1230. ^o Kurmoo, M.; Clark, R. J. H. *Inorg. Chem.* **1985**, *24*, 4420. ^p The F values have been estimated using equations related to M–M–X systems: $\lambda_1 + \lambda_3 = F(M_2) (1/m_X + 1/m_M) + 2F(MX)/m_M$ and $\lambda_1\lambda_3 = (2m_M + m_X)/m_X m_M^2$. Using $\nu(\text{PtX}) = 291$ and 210 cm^{-1} for X = Cl and Br, respectively (see ref o), the resolution of the quadratic equations leads to two solutions. The one that was physically meaningless was rejected. ^q Clark, R. J. H.; Kurmoo, M.; Dawes, H. M.; Hursthouse, M. *Inorg. Chem.* **1986**, *25*, 409. ^r Che, C.-M.; Herstein, F. M.; Schaefer, W. P.; Marsh, R. E.; Gray, H. B. *J. Am. Chem. Soc.* **1983**, *105*, 4604. ^s Alexander, K. A.; Stein, P.; Hedden, D. B.; Roundhill, D. M. *Polyhedron* **1983**, *2*, 1389. ^t The F values have been estimated using equations related to X–M–M–X systems: $\lambda_1\lambda_2 = 2F(M_2)F(MX)/m_X m_X$ and $\lambda_1 + \lambda_2 = 2F(M_2)/m_M + (1 + m_X/m_M)F(MX)/m_X$ (Herzberg, G. *Vibrational Spectra of Polyatomic Molecules*; Van Nostrand: Princeton, NJ, 1950; Vol II). For Pt₂(pop)₄(NO₂)₂⁴⁻, $\nu(\text{Pt–N}) = 297 \text{ cm}^{-1}$ (ref s) and $m_X = 46 \text{ g/mol}$. For Pt₂(pop)₄Br₂⁴⁻, $\nu(\text{Pt–Br}) = 224 \text{ cm}^{-1}$ (ref u). For Pt₂(pop)₄Cl₂⁴⁻, $\nu(\text{Pt–Cl}) = 304 \text{ cm}^{-1}$. For Pt₂(dppm)₂Cl₂, $\nu(\text{Pt–Cl}) = 271 \text{ cm}^{-1}$ (ref x). For Pt₂(CO)₂Cl₄²⁻, $\nu(\text{Pt–Cl}) = 272 \text{ cm}^{-1}$ (ref z). ^y Che, C.-M.; Lee, W.-M.; Mak, T. C. W.; Gray, H. B. *J. Am. Chem. Soc.* **1986**, *108*, 4446. ^z Stein, P.; Dickson, M. K.; Roundhill, D. M. *J. Am. Chem. Soc.* **1983**, *105*, 3489. ^{aa} Alexander, K. A.; Bryan, S. A.; Fronczek, F. R.; Fultz, W. C.; Rheingold, A. L.; Roundhill, D. M.; Stein, P.; Watkins, S. F. *Inorg. Chem.* **1984**, *24*, 2803. ^{ab} Alves, O. L.; Vitorge, M.-C.; Sourisseau, C. *Now. J. Chim.* **1983**, *7*, 231. ^{ac} Brown, M. P.; Puddephatt, R. J.; Rashidi, M.; Manojlovic-Muir, L. J.; Muir, K. W.; Solomon, T.; Seddon, K. R. *Inorg. Chim. Acta* **1977**, *23*, L33. Manojlovic-Muir, L. J.; Muir, K. W.; Solumun, T. *Acta Crystallogr.* **1979**, *B35*, 1237. ^{ad} Goggin, P. L.; Goodfellow, R. J. *J. Chem. Soc., Dalton Trans.* **1973**, 2355. ^{ae} Modinos, A.; Woodward, P. J. *J. Chem. Soc., Dalton Trans.* **1974**, 1516. ^{bb} Jansson, K.; Scullman, R. J. *Mol. Spectrosc.* **1976**, *61*, 299.

($\nu(\text{PtCl})$). The 38-cm⁻¹ peak now appears as a weak shoulder near the Raleigh line. The region above 500 cm⁻¹ (as well as the IR spectra) was not investigated, except to measure $\nu(\text{CN})$ (2217 cm⁻¹; strong and relatively broad).

Compound 6 forms a linear chain ($r(\text{Pt}\cdots\text{Pt}) = 4.221 \text{ Å}$)⁴⁵ and belongs to a family of extremely weak interacting M₂ species. Such examples have already been characterized: [cis-Pd(CNC-(CH₃)₃)₂Cl₂]₂ ($r(\text{Pd}_2) = 4.42(6) \text{ Å}$, $\nu(\text{Pd}_2) = 19 \text{ cm}^{-1}$)^{32a} and Rh₂(dmb)₄²⁺ ($r(\text{Rh}_2) = 4.4 \text{ Å}$, $\nu(\text{Rh}_2) = 26 \text{ cm}^{-1}$; dmb = 1,8-diisocyno-*p*-menthane).⁴⁶ Again no resonance Raman investigation was possible, as the samples were colorless. Previous examples of a series of [cis-Pd(CNR)₂Cl₂]₂ complexes where $r(\text{Pd}_2)$ varies with R have shown that $\nu(\text{Pd}_2)$ could easily be assigned by monitoring $\nu(\text{Pd}_2)$ vs $r(\text{Pd}_2)$.^{32a} This approach could not be used in this work.⁴⁷ Using Table 4 data for which $3.61 < r(M_2) < 4.36 \text{ Å}$, one can tentatively predict that $\nu(M_2)$ should be $\sim 20 \text{ cm}^{-1}$. Figure 8 shows the Raman spectrum of compound 6, where no peak is seen at $\sim 20 \text{ cm}^{-1}$. Rather, a single (and only) peak is reproducibly observed at 5 cm^{-1} (uncertainty = $\pm 1 \text{ cm}^{-1}$), a peak that would strongly appear as a low-frequency lattice mode. One can calculate $\nu(\text{Pt}_2)$ using a reparametrized Herschback–Laurie relationship between $r(\text{Pt}_2)$ and $F(\text{Pt}_2)$ (H–L: $r(M_2) = a \ln F(M_2) + b$; F in mdyn Å⁻¹).^{32,33b} Using this work's data (compounds 1, 3, 4, and 5) combined with 12 other

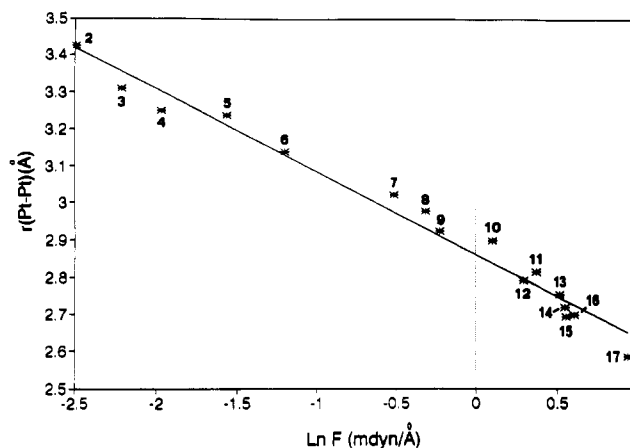


Figure 9. Graph of $r(\text{Pt}_2)$ vs $\ln F(\text{Pt}_2)$.

literature ones for which both $r(\text{Pt}_2)$ and $\nu(\text{Pt}_2)$ are known (Table 5), a reparametrized H–L equation applied to Pt systems is designed (Figure 9):

$$r(\text{Pt}_2) = -0.223 \ln F(\text{Pt}_2) + 2.86 \quad (1)$$

The coefficient correlation (σ) is 0.98 (for 16 data points). Using $r(\text{Pt}_2) = 4.22 \text{ Å}$, eq 1 predicts that $F(\text{Pt}_2) = 0.0022 \text{ mdyn } \text{Å}^{-1}$. $\nu(\text{Pt}_2)$ can be extracted from $\nu = (2\pi c)^{-1}(F/m)^{1/2}$ (c = speed of light; m = mass) and is found to be 4.2 cm^{-1} ! This agreement allows the assignment of the 5-cm^{-1} peak to $\nu(\text{Pt}_2)$ for compound 6. This mode is obviously a lattice mode along the Pt chain. The $F(\text{Pt}_2)$ value ($0.0027 \text{ mdyn } \text{Å}^{-1}$) is significantly lower than those reported in Table 4. When this datum is added to the list designed

(45) Melanson, R.; Hubert, J.; Rochon, F. D. *Acta Crystallogr.* **1976**, *B32*, 1974.

(46) Miskowski, V. M. Unpublished results. See also footnote 13 in: Perreault, D.; Drouin, M.; Michel, A.; Harvey, P. D. *Inorg. Chem.* **1992**, *31*, 2740.

(47) The Pt(CN)₄²⁻ salts provide samples with $r(\text{Pt}\cdots\text{Pt})$ values around 3.4 and 3.7 Å¹² but turn out to be as strongly luminescent (as for compound 2) as those reported in ref 21, preventing successful Raman measurements.

Table 6. Comparison of the H–L Parameters with $E_{\text{diss}}(\text{M}_2)$

element	H–L		σ	no. of data points	ref	$E_{\text{diss}}(\text{M}_2)/\text{kJ mol}^{-1}$	ref
	slope ^a	intercept					
Ag	-0.284 (0.025)	2.53 (0.08)	0.95	9	28a	159 ± 6	49a,b
Pd	-0.387 (0.013)	2.67 (0.07)	0.99	12	28a	105 ± 21	49c
Rh	-0.287 (0.019)	2.78 (0.06)	0.96	14	unpublished ^b	282 ± 21 ^c	49d
Au	-0.290 (0.019)	2.68 (0.07)	0.96	11	28b	221 ± 2	49e
Pt	-0.223 (0.009)	2.86 (0.04)	0.98	16	this work	358 ± 15	49f,g

^a The values in parentheses are the standard deviations. ^b Harvey, P. D.; Shafiq, F.; Eisenberg, R. Submitted for publication (see footnote 42). ^c This value accounts for the cleavage of a triple bond (see ref 50).

for eq 1, the H–L parameters (slope and intercept) remain the same within the experimental uncertainty and σ becomes 0.99.

Comments on the H–L Equation. Previous works³² suggested the use of reparametrized H–L equations applied to each individual element (when available), in order to gain “accuracy” in the analysis. Historically, Badger’s rules^{33a} ($r = a + b(F^{-1/3})$) were improved by the H–L rules^{33b} ($r = a + b \log F$), which in their turn were improved by Woodruff’s rules ($r = a + b \exp(-F/c)$).^{33c–e} These rules were all designed for each single-row element. The major criticism for Woodruff’s rules was that the equations become inaccurate at distances approaching $r \rightarrow a + b$ and become inadequate for $r(\text{M}_2)$ values larger than the sum of $a + b$.³² The comparison of Woodruff’s rule for the fifth-row element ($r(5d) = 2.04 + 1.32 \exp(-F/2.17)$)^{33e} with eq 1 shows that Woodruff’s rule also surprisingly deviates greatly from the experimental values in the shorter Pt–Pt bond region (Table 9, available in the supplementary material). The differences (Δ) between the calculated (eq 1) and the experimental data are well within $\pm 0.05 \text{ \AA}$. Two exceptions occur: compound **6** ($r(\text{Pt}_2) = 4.22 \text{ \AA}$, $\Delta = 0.10 \text{ \AA}$, 2.4% error) and $\text{Pt}_2(\text{CO})_2\text{Cl}_4^{2-}$ ($r(\text{Pt}_2) = 2.584 \text{ \AA}$, $\Delta = 0.07 \text{ \AA}$, 2.7% error). This is due to the difficulty of evaluating $F(\text{Pt}_2)$ in some cases. Nevertheless, the error bar when eq 1 is used is $\pm 0.05 \text{ \AA}$.

The H–L empirical parameters are element-dependent (Table 6), and with the addition of the Pt element to the existing list (Pd, Ag, Au),³² one can make some correlation between these parameters and existing properties of the element. The intercept values going from row 4 to row 5 predictably increase due to the increase in atomic radii.⁴⁸ On the other hand, the intercepts increase with the atomic number, which somewhat contradicts the trend associated with the ionic radii.^{20,48} This behavior is not understood at this time.

Surprisingly, the slope in the force constant relation for the Pd_2 system is greater than that for Pt_2 , while the slope values are essentially identical for the Ag_2 and Au_2 systems. A high slope (in this case -0.387 for Pd_2 species) indicates that the $F(\text{M}_2)$ values are very sensitive to $r(\text{M}_2)$, which means that attractive interactions disappear quickly with the increase in $r(\text{M}_2)$. In principle, a molecule such as Pd_2 should be easy to dissociate. Indeed, for a same-row element, a high slope is associated with a small dissociation energy (E_{diss}) of the diatomic molecule,⁴⁹ and vice versa (see Table 6 for details). In the Rh_2 case, the slope (-0.287) suggests that $E_{\text{diss}}(\text{Rh}_2) \sim E_{\text{diss}}(\text{Ag}_2)$. This is not the case, since $E_{\text{diss}}(\text{Rh}_2)$ is larger and accounts for the cleavage of a triple bond.⁵⁰ For the Ag_2 and Au_2 systems, the slopes are also

the same (within the experimental uncertainty), suggesting that $E_{\text{diss}}(\text{Ag}_2) \sim E_{\text{diss}}(\text{Au}_2)$. Experimentally, this is not the case: $E_{\text{diss}}(\text{Ag}_2) < E_{\text{diss}}(\text{Au}_2)$.^{49a,b,e} A reasonable and tentative explanation for this trend is the presence of relativistic effects which increase the strength (accompanied by shrinkage) of the Au–Au bond.⁵¹

Summary. The resonance Raman experiments for compound **1** are consistent with the IL assignment²⁴ for the lowest energy band and consistent with the $d\sigma \rightarrow p\sigma^*$ one in compound **4**. For the first time, the $\nu(\text{Pt}_2)$ values for Pt_2 species where $r(\text{Pt}_2) > 3.2 \text{ \AA}$ were obtained, which turned out to be $< 100 \text{ cm}^{-1}$, as previously predicted.²² In one case (chain compound, compound **2**), the Raman data could not be obtained, but we were able to propose a $\nu(\text{Pt}_2)$ assignment based upon the IR-active mode. Using the reparametrized H–L equation, $\nu(\text{Pt}_2)$ for the chain compound **6** is assigned at 5 cm^{-1} ($r(\text{Pt}\cdots\text{Pt}) = 4.22 \text{ \AA}$), the lowest value ever reported for $\nu(\text{M}_2)$. Such a $\nu(\text{M}_2)$ value is characteristic of weakly interacting dimers (such as the van der Waals dimers; see $\text{HeXe}(\Sigma^+)$, $\nu = 8.2 \text{ cm}^{-1}$).⁸ This mode is essentially a lattice mode along the Pt chain. Finally, the comparison of the H–L parameters (slopes and intercepts) for the Ag_2 , Pd_2 , Rh_2 , Au_2 , and Pt_2 systems allows correlations with some physical properties such as the atomic radii and $E_{\text{diss}}(\text{M}_2)$ of a single bond. If these correlations turn out to be general for most elements, one can predict qualitatively, $E_{\text{diss}}(\text{M}_2)$ if such a datum is not already available.

Acknowledgment. This research was supported by the NSERC and the FCAR. P.D.H. thanks Mr. S. Burnett (McGill University) for recording some of the spectra and Professor F. Rochon (Université du Québec à Montréal) and Professor F. Faraone (Università di Messina) for the generous gifts of compounds **6** and **5**, respectively.

Supplementary Material Available: Tables giving crystal data and details of the structure determination, all atomic coordinates, bond distances, bond angles, anisotropic thermal parameters, and torsional angles for **4** and a comparison of the calculated (Woodruff’s rule, H–L) and the experimental $r(\text{Pt}_2)$ values (18 pages). Ordering information is given on any current masthead page.

(48) $r_{\text{vdw}} = 1.60, 1.70, 1.70\text{--}1.80,$ and 1.70 \AA for Pd, Ag, Pt, and Au, respectively, and r_{ion} (ionic radii) = 1.08 and 1.51 \AA for Ag^+ and Au, respectively.²⁰

- (49) (a) Gurvich, L. V.; Karachevstev, G. V.; Kondratyev, V. N.; Lebedev, Y. A.; Mendredev, V. A.; Papapov, V. K.; Khodeen, Y. S. *Bond Energies, Ionization Potentials and Electron Affinities*; Nauka: Moscow, 1974 (in Russian). (b) Gale, J. L. In *Metal Clusters*; Moskovits, M., Ed.; Wiley, Toronto, 1986; p 136. (c) Gingerich, K. A. *J. Cryst. Growth* **1971**, *9*, 31. (d) Gingerich, K. A.; Gupta, S. K. *J. Chem. Phys.* **1978**, *69*, 505. (e) Kordish, J.; Gingerich, K. A.; Seyse, R. *J. Chem. Phys.* **1974**, *61*, 5514. (f) Gingerich, K. A.; Cocke, D. L.; Miller, F. *J. Chem. Phys.* **1976**, *64*, 4027. (g) Gupta, S. K.; Nappi, B. M.; Gingerich, K. A. *Inorg. Chem.* **1981**, *20*, 966.
- (50) Goursoot, A.; Papai, I.; Salahub, D. R. *J. Am. Chem. Soc.* **1992**, *114*, 7452.
- (51) Pyykko, P. *Chem. Rev.* **1988**, *88*, 563.